1521-0103/353/2/405–414$25.00
THE JOURNAL OF PHARMACOLOGY AND EXPERIMENTAL THERAPEUTICS

http://dx.doi.org/10.1124/jpet.114.221176
J Pharmacol Exp Ther 353:405–414, May 2015

The Journal of PHARMACOLOGY And Experimental Therapeutics

VX-509 (Decernotinib) Is a Potent and Selective Janus Kinase 3 Inhibitor That Attenuates Inflammation in Animal Models of Autoimmune Disease[S]

Sudipta Mahajan, James K. Hogan, Dina Shlyakhter, Luke Oh, Francesco G. Salituro, Luc Farmer, and Thomas C. Hoock

Departments of Integrated Biology and Chemistry, Vertex Pharmaceuticals, Boston, Massachusetts (S.M., J.K.H., D.S., L.F., T.C.H.); Sage Therapeutics, Cambridge, Massachusetts (F.G.S.); and Mallinckrodt Pharmaceuticals, Ellicott City, Maryland (L.O.)

Received November 10, 2014; accepted March 10, 2015

ABSTRACT

Cytokines, growth factors, and other chemical messengers rely on a class of intracellular nonreceptor tyrosine kinases known as Janus kinases (JAKs) to rapidly transduce intracellular signals. A number of these cytokines are critical for lymphocyte development and mediating immune responses. JAK3 is of particular interest due to its importance in immune function and its expression, which is largely confined to lymphocytes, thus limiting the potential impact of JAK3 inhibition on nonimmune physiology. The aim of this study was to evaluate the potency and selectivity of the investigational JAK3 inhibitor VX-509 (decernotinib) [(*R*)-2-((2-(1*H*-pyrrolo[2,3-*b*]pyridin-3-yl)pyrimidin-4-yl)amino)-2-methyl-*N*-(2,2,2-trifluoroethyl)butanamide] against JAK3 kinase activity and inhibition of JAK3-mediated signaling in vitro and JAK3-dependent physiologic processes in vivo. These results demonstrate that VX-509 potently inhibits JAK3 in enzyme assays (K_i = 2.5 nM + 0.7 nM) and cellular assays dependent on JAK3 activity (IC_{50} range, 50–170 nM), with limited or no measurable potency against other JAK isotypes or non-JAK kinases. VX-509 also showed activity in two animal models of aberrant immune function. VX-509 treatment resulted in dose-dependent reduction in ankle swelling and paw weight and improved paw histopathology scores in the rat collagen-induced arthritis model. In a mouse model of oxazolone-induced delayed-type hypersensitivity, VX-509 reduced the T cell–mediated inflammatory response in skin. These findings demonstrate that VX-509 is a selective and potent inhibitor of JAK3 in vitro and modulates proinflammatory response in models of immune-mediated diseases, such as collagen-induced arthritis and delayed-type hypersensitivity. The data support evaluation of VX-509 for treatment of patients with autoimmune and inflammatory diseases such as rheumatoid arthritis.

Introduction

Despite significant advances in therapies for the treatment of many autoimmune diseases, such as rheumatoid arthritis (RA), a persistent unmet need still exists for more effective, durable, and convenient treatment options. Cytokines are critical regulators of immunity and inflammation and are important contributors to the pathology underlying autoimmune diseases such as RA (Carmona et al., 2010; McInnes and Schett, 2011). Cellular responses to cytokines, certain hormones, and growth factors are mediated by cytoplasmic nonreceptor tyrosine kinases called Janus kinases (JAKs) (Ihle and Kerr, 1995; Kiu and Nicholson, 2012). When bound to their cell surface receptors, cytokines from the class I and class II cytokine superfamilies activate one or more members of the intracellular JAK family, of which there are four, as follows: JAK1, JAK2, JAK3, and tyrosine kinase (TYK)2 (Ihle and Kerr, 1995; Kiu and Nicholson, 2012). JAKs are activated via auto- or transphosphorylation of their partner JAK. Ultimately, JAKs and subsequently signal transducers and activators of transcription (STATs) regulate expression of cytokine-induced target genes, impacting a variety of physiologic processes (Darnell et al., 1994; Darnell, 1997; Stark and Darnell, 2012). Different combinations of JAKs and STATs control distinct biologic functions, depending on the type of cytokine receptor with which they associate (Ihle and Kerr, 1995; Kiu and Nicholson, 2012). Although the common γ-chain cytokines [interleukin (IL)-2, IL-4, IL-7, IL-9, IL-15, and IL-21] signal via JAK3 and JAK1, the gp130 family of cytokines (IL-6, IL-11, IL-13, IL-27, leukemia inhibitory factor, ciliary neurotrophic factor, etc.) signals via JAK1, JAK2, and TYK2. Similarly, type I interferons (IFN) signals using the JAK-1/TYK2 pairs, erythropoietin (EPO), granulocyte macrophage colony-stimulating factor (GM-CSF), IL-3,

This work was sponsored by Vertex Pharmaceuticals.
dx.doi.org/10.1124/jpet.114.221176.
[S] This article has supplemental material available at jpet.aspetjournals.org.

ABBREVIATIONS: ANOVA, analysis of variance; BSA, bovine serum albumin; CFU-E, colony-forming unit–erythroid; CIA, collagen-induced arthritis; CII, type II collagen; DMSO, dimethylsulfoxide; DTH, delayed-type hypersensitivity; DTT, dithiothreitol; EPO, erythropoietin; GM-CSF, granulocyte macrophage colony-stimulating factor; HPLC, high-performance liquid chromatography; IFN, interferon; IL, interleukin; JAK, Janus kinase; MLR, mixed-lymphocyte reaction; PBS, phosphate-buffered saline; polyE4Y, poly(glutamate)$_4$tyrosine; PRED, prednisolone; RA, rheumatoid arthritis; STAT, signal transducers and activators of transcription; TCA, trichloroacetic acid; TYK, tyrosine kinase; VX-509, (*R*)-2-((2-(1*H*-pyrrolo[2,3-*b*]pyridin-3-yl)pyrimidin-4-yl)amino)-2-methyl-*N*-(2,2,2-trifluoroethyl)butanamide.

and IL-5 primarily use JAK2, and IFN-γ signals via JAK1/JAK2.

JAK1 and JAK2 are broadly used across a variety of tissue and cell types. Knockout of either the JAK1 or JAK2 gene has lethal consequences (Neubauer et al., 1998; Parganas et al., 1998; Rodig et al., 1998); JAK1 knockout mice are viable but die early in the postnatal period, which is hypothesized to be a result of impaired neural development related to the lack of gp130 receptor signaling (Rodig et al., 1998). JAK2 is solely responsible for EPO signaling, and knockout of this gene results in lethal anemia (Neubauer et al., 1998). In contrast, JAK3 knockout mice are viable and have defects only in immune cell development (Nosaka et al., 1995; Park et al., 1995; Grossman et al., 1999). The expression of JAK3 is largely restricted to lymphocytes, where it binds exclusively to the common γ-chain of the receptors for IL-2, -4, -7, -9, -15, and -21 (Ghoreschi et al., 2009). JAK3 controls the survival and proliferation of lymphocytes as a part of host defense, and in the context of autoimmune diseases, by signaling through the γ-chain family of cytokines (Ghoreschi et al., 2009; O'Shea and Plenge, 2012). JAK3 mutations in humans have been shown to cause significant impairments in B and T cell function as well, demonstrating a parallel and targeted role for JAK3 in human immune response (Macchi et al., 1995; Russell et al., 1995; Taylor et al., 1996; Cacalano et al., 1999). Thus, inhibiting JAK3 is an attractive intervention point at which to develop therapies for a variety of immune-mediated diseases such as RA, and may spare important signaling in other JAK pathways.

The objective of this study was to characterize VX-509 (decernotinib) [(*R*)-2-((2-(1*H*-pyrrolo[2,3-*b*]pyridin-3-yl)pyrimidin-4-yl)amino)-2-methyl-*N*-(2,2,2-trifluoroethyl)butanamide], an oral selective JAK3 inhibitor, using enzymatic, cellular, and animal models of immune function. The results show that VX-509 exhibits robust and selective inhibition of JAK3 in vitro and ability to ameliorate immune-mediated defects in autoimmune disease models, providing a solid rationale for pursuing clinical studies of VX-509 as therapy for human autoimmune diseases.

Materials and Methods

Drugs, Cells, and Reagents

VX-509 (mol. wt. = 392.38) was synthesized at Vertex Pharmaceuticals (Boston, MA) (Fig. 1) (L. Farmer et al., submitted manuscript). HT-2, TF-1, and HeLa cells were obtained from American Type Culture Collection (Manassas, VA); IL-2, GM-CSF, IL-4, and CD40L were purchased from R&D Systems (Minneapolis, MN); phospho–STAT-5 phycoerythrin from BD Biosystems (San Jose, CA); phytohemagglutinin from Sigma-Aldrich (St. Louis, MO); human B cells from AllCells (Emeryville, CA); Roswell Park Memorial Institute medium tissue culture medium, phosphate-buffered saline (PBS), and 10,000 U/ml penicillin-streptomycin from Life Technologies (Grand Island, NY); fetal bovine serum from Thermo Fisher Scientific (Waltham, MA); Cellomics STAT-2 activation high content screening reagent kits from Pierce Biotechnology/Thermo Scientific (Rockford, IL); Freund's incomplete adjuvant from Difco (Detroit, MI); bovine type II collagen from Elastin Products (Owensville, MO); pyruvate kinase, lactate dehydrogenase, phosphoenolpyruvate, ATP, poly(glutamate)$_4$tyrosine (polyE4Y), bovine serum albumin (BSA), myelin basic protein, and IFN-α from Sigma-Aldrich; ^{33}P-γ-ATP, GF/B filter plates, and Ultima Gold scintillant from PerkinElmer Life Sciences (Boston, MA); peptide substrates from American Peptide (Sunnyvale, CA); and dimethylsulfoxide (DMSO) from American Type Culture Collection. JAK3 and other kinases were expressed and purified using standard recombinant methods at Vertex Pharmaceuticals (Boston, MA).

In Vitro Experiments

Kinase Activity Assays. The effect of VX-509 on JAK3 activity was assessed by measuring the residual kinase activity of the recombinantly expressed JAK3 kinase domain using a radiometric assay. The final concentrations of the components in the assay were as follows: 100 mM HEPES (pH 7.5), 10 mM $MgCl_2$, 1 mM dithiothreitol (DTT), 0.01% BSA, 0.25 nM JAK3, 0.25 mg/ml polyE4Y, and 5 μM ^{33}P-γ-ATP (200 μCi/μmol). A 10 mM stock solution of VX-509 was prepared in DMSO, from which additional dilutions were prepared. A substrate mixture (100 mM HEPES, 10 mM $MgCl_2$, 0.5 mg/ml polyE4Y, and 10 μM ^{33}P-γ-ATP) was added and mixed with VX-509 stock solution. The reaction was initiated by the addition of an enzyme mixture [100 mM HEPES (pH 7.5), 10 mM $MgCl_2$, 2 mM DTT, 0.02% BSA, 0.5 nM JAK3]. After 15 minutes, the reaction was quenched with 20% trichloroacetic acid (TCA). The quenched reaction was transferred to the GF/B filter plates and washed three times with 5% TCA. Following the addition of Ultimate Gold scintillant (50 μl), the samples were counted in a Packard TopCount gamma counter (PerkinElmer). In this procedure, the radioactivity trapped is a measure of the residual JAK3 kinase activity. From the activity versus concentration of VX-509 titration curve, the K_i value was determined by fitting the data to an equation for competitive tight binding inhibition kinetics using Prism software (version 4.0; GraphPad Software, San Diego, CA).

The Effect of VX-509 on the Activity of Other Kinases. The selectivity of VX-509 against the other JAK isozymes and other non-JAK protein kinases was determined. The assay format (spectrophotometric or radiometric) and ATP and peptide concentrations used in each assay are shown in Supplemental Table 1. Radiometric assays were performed in the same manner as described for JAK3. Spectrophotometric assays were performed using a standard coupled-enzyme assay used for kinases, one similar to that described by Chen et al. (2000). Briefly, each mole of ADP produced by the protein kinase–catalyzed reaction is coupled to the generation of 1 mol NAD^+ from NADH using pyruvate kinase and lactate dehydrogenase. The final concentrations of the components in the assay were as follows: 100 mM HEPES (pH 7.5), 10 mM $MgCl_2$, 1 mM DTT, 2.5 mM phosphoenolpyruvate, 200 μM NADH, 50 μg/ml pyruvate kinase, 10 μg/ml lactate dehydrogenase, and ATP and protein/peptide substrates, as shown in Supplemental Table 1.

KinaseProfiler assays were performed at Upstate Discovery (Scotland, UK), a subsidiary of EMD Millipore (Billerica, MA). All assays employed radiometric detection in the manner described by Davies et al. (2000). Supplemental Table 2 lists the peptide substrate, its concentration, and the concentration of ATP used in each kinase assay. VX-509 was solubilized in DMSO and added to the assay solutions to a final concentration of 2 μM. The reaction was quenched with 20% TCA, and the ^{33}P-labeled phospho-peptide/protein produced was trapped on a filter and quantified using a radioactivity counter.

In Vitro Cell-Based Selectivity Assays

Preparation of VX-509 for Selectivity Studies. VX-509 was serially diluted in DMSO as eight 1:3 dilutions starting from 10 mM. Dilutions of VX-509 in DMSO were added to medium (Roswell Park Memorial Institute medium, 10% fetal bovine serum, 100 U/ml penicillin-streptomycin) to make a 2× solution; this solution was then added to the cells to achieve VX-509 concentrations between and 4.5 nM and 10 μM.

Phosphorylated STAT-5 Flow Cytometric Analysis. HT-2 or TF-1 cells were deprived of growth factors for 4 hours at 37°C. Cells were plated in 96-well plates at a density of 2.5×10^5 cells/well (50 μl 5×10^6 cells/ml stock). VX-509 solution was plated in triplicate, in columns, at final concentrations ranging from 10 μM to 4.5 nM. Two

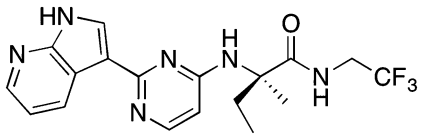

Fig. 1. Chemical structure of VX-509 (decernotinib).

columns of cells were plated with DMSO as the proliferation control. The cells were incubated at 37°C for 1 hour, after which cells in the VX-509 columns and cells in one of the control columns were stimulated with either IL-2 (HT-2 cells) for 20 minutes, or GM-CSF (TF-1 cells) for 15 minutes, at 37°C. The second column of cells was not stimulated and served as the negative control. Plates were centrifuged at 500*g* for 5 minutes, and the supernatant was aspirated. Cells were fixed with 4% formaldehyde for 10 minutes at room temperature. Plates were centrifuged, and the supernatant was aspirated. Cells were then permeabilized by incubation in 90% methanol for 30 minutes at 4°C. Plates were centrifuged at 500*g* for 5 minutes, and the supernatant was aspirated. Plates were washed by adding PBS and immediately centrifuging at 500*g* for 5 minutes, after which the supernatant was aspirated. Cells were stained with a 1:10 dilution of anti–phospho-STAT-5 phycoerythrin antibody for 45 minutes on a shaker at room temperature. Cells were then washed by adding PBS, centrifuging plates for 5 minutes at 500*g*, and aspirating the supernatant. Cells were resuspended in PBS, and STAT-5 phosphorylation was quantified on a Guava PCA 96 fluorescence-activated cell-sorting reader (EMD Millipore). The IC_{50} of VX-509 was determined using Softmax pro software.

STAT-2 Nuclear Translocation Assay. HeLa cells were plated in a 96-well plate at a density of 5×10^3 cells/well. The plates were incubated at 37°C for 18 hours (overnight) in a CO_2 incubator. VX-509 was added to plates at a final concentration ranging from 4.5 nM to 10 μM, and the plates were placed in a CO_2 incubator at 37°C for 1 hour. Cells were then stimulated with IFN-α and incubated for 45 minutes at 37°C in a CO_2 incubator (medium only for negative control plates). Plates were processed according to the protocol from the Cellomics STAT-2 activation HitKit and screened using the ArrayScan II High Content Screening System (Beckman Coulter, Fullerton, CA). Data were analyzed using Softmax pro software to generate an IC_{50} value for VX-509.

In Vitro JAK2- and JAK3-Dependent Functional Assay

Preparation of VX-509 for Functional Assays. VX-509 (10 mM) was serially diluted in DMSO as six 1:4 dilutions. Each of the DMSO dilutions was added to complete medium and then to the cells in the mixed-lymphocyte reaction (MLR), T-cell blast proliferation assays, or B-cell proliferation assay, giving a range of final concentrations between 9.7 nM and 10 μM.

MLR Assay. Spleens from 8- to 10-week-old female mice (CBA and BALB/c; Jackson ImmunoResearch Laboratories, West Grove, PA) were used to isolate splenocytes. The splenocytes from each strain of mouse were plated at a density of 1.8×10^5 cells/well in 96-well plates. The VX-509 dilutions were added to the wells; two rows were plated with DMSO alone and served as the proliferation controls for the assay. The plates were incubated at 37°C in a CO_2 incubator for 4 days. On day 5, 20 μCi/ml methyl-[^{3}H]thymidine was added to each well. After 7 hours, cells were harvested onto Betaplate double filters using a TOMTEC Harvester 96. Filters were dried for 1 hour, and then 20 ml scintillation fluid was added to each filter. Filters were analyzed for radioactive counts on a PerkinElmer-Wallace beta counter (1205 Betaplate Beta Liquid Scintillation Counter). Data were analyzed to generate an IC_{50} value using Softmax pro software.

TABLE 1
JAK3-dependent cell assays (*n* for each assay provided in the table)

Assay	JAK Isoform Dependency	IC_{50} ± S.D.	*n*
		nM	
IL-2–stimulated HT-2 STAT-5 phosphorylation	JAK3	99 ± 40	4
Mouse two-way MLR	JAK3	170 ± 101	4
Human T-cell blast proliferation	JAK3	140, 400	2
CD40L/IL-4–induced B-cell proliferation	JAK3	50	1

IL-2–Stimulated Human T-Cell Blast Proliferation Assay. Whole-blood samples from healthy volunteers were used to collect peripheral blood mononuclear cells, which were plated in T75 tissue culture flasks at a density of 1×10^6/ml. Cells were stimulated with 10 μg/ml phytohemagglutinin at 37°C for 72 hours. After 72 hours, cells were detached from the flask by scraping, washed, and plated at a density of 1×10^5/well in a 96-well plate. VX-509 (9.7 nM to 10 μM) was added, and plates were incubated for 30 minutes at 37°C, followed by stimulation with human IL-2. In two rows, only DMSO was added; one row was not stimulated with IL-2, and one row was stimulated with IL-2 to serve as the proliferation control. Plates were incubated at 37°C for 2 days. On day 2, cells were pulsed with 20 μCi/ml methyl-[^{3}H]thymidine for 18–24 hours and harvested onto filters for radiographic determination using a PerkinElmer-Wallace beta counter (1205 Betaplate Beta Liquid Scintillation Counter). Data were analyzed to generate an IC_{50} value using Softmax pro software.

CD40L/IL-4–Induced B-Cell Proliferation Assay. Frozen purified human B cells were thawed, washed, and resuspended in complete medium. Cells were plated onto a 96-well plate at a density of 2×10^5 cells/well. VX-509 was added, and plates were incubated for 30 minutes at 37°C, followed by stimulation with a combination of 10 ng/ml IL-4 and 1 μg/ml CD40L. DMSO alone was added to the top two rows, one of which was stimulated with IL-4 or CD40L (negative control) and the other of which served as a proliferation control. The plates were incubated at 37°C for 6 days. On day 6, cells were pulsed with [^{3}H]thymidine for 7 hours and harvested onto filters for radioactive determination using a PerkinElmer-Wallace beta counter (1205 Betaplate Beta Liquid Scintillation Counter). Data were analyzed with Softmax pro software to generate an IC_{50} value.

Colony-Forming Unit–Erythroid Assay. Colony-forming unit–erythroid (CFU-E) assays were performed by StemCell Technologies (Vancouver, BC, Canada). Briefly, clonogenic progenitors from normal human bone marrow of the erythroid, myeloid, and multipotential lineages were plated in methylcellulose-based media formulations containing 50 ng/ml stem cell factor, 10 ng/ml GM-CSF, 10 ng/ml IL-3, and either 3.0 or 0.3 U/ml EPO. VX-509 was added to produce final concentrations between 0.01 and 10 μM. Solvent control cultures, as well as standard controls, were also made for each media formulation. The cultures were performed in triplicate at 1×10^4 cells per culture. Following 14 days in culture, the colonies were classified based on size and cell and colony morphology.

In Vivo Studies

VX-509 Preparation for In Vivo Studies. VX-509 was solubilized at 2, 5, and 10 mg/ml as an aqueous solution in 10% vitamin E D-α-tocophenyl polyethylene glycol 1000 succinate and 1% hydroxypropyl methylcellulose acetyl succinate. VX-509 powder and vehicle were mixed by vortexing for 2–3 minutes, then placed in an ultrasonic water bath at room temperature for up to 30 minutes, and finally kept stirring at room temperature until dosing.

Animal Care for In Vivo Studies. Rats and mice were housed in groups of four or five in polycarbonate cages with wood chip bedding, on a 12-hour light/dark cycle. Food and water were suspended from wire cage tops and available ad libitum. Animals were given at least 7 days to acclimate to the laboratory before testing. All studies were performed in compliance with the regulations of the Institutional Animal Care and Use Committee.

Collagen-Induced Arthritis Model in the Rat. The study was conducted at Bolder BioPATH (Boulder, CO). The collagen-induced arthritis (CIA) model shares a number of pathologic, genetic, and

TABLE 2
Non-JAK3–dependent cell assays (n for each assay provided in the table)

Assay	JAK Isoform Dependency	IC_{50} ± S.D.	n
		nM	
GM-CSF–stimulated TF-1 STAT-5 phosphorylation	JAK2	2590 ± 1600	4
IFN-α–stimulated HeLa STAT-2	JAK1, TYK2	11,900 ± 3651	3
CFU-E 3 U/ml EPO	JAK2	12,000, 3300	2
CFU-E 0.3 U/ml EPO	JAK2	7800, 2700	2

immunologic features with RA. Therefore, the CIA rat model was used to evaluate the effects of oral VX-509 [10 mg/kg b.i.d., 25 mg/kg b.i.d., 50 mg/kg b.i.d., 50 mg/kg q.d., or 100 mg/kg q.d.] on joint inflammation and histopathology. Female Lewis rats (157–187 g) were obtained from Charles River Laboratories (Wilmington, MA) or Harlan (Indianapolis, IN). On days 0 and 6, animals were anesthetized with isoflurane and injected with 300 μl Freund's incomplete adjuvant, containing 2 mg/ml bovine type II collagen, at the base of the tail and two sites on the back. The rats were randomized to study groups at the onset of paw swelling (arthritis), which occurred between days 10 and 11. Dosing of either VX-509 or vehicle via oral gavage was initiated on the first day of established arthritis and continued to day 6 of arthritis. Dosing volume was 5 ml/kg. Groups were controls (no collagen injection plus vehicle; $n = 4$), collagen plus vehicle ($n = 5$), collagen plus VX-509 10 mg/kg b.i.d. ($n = 8$); collagen plus VX-509 25 mg/kg b.i.d. ($n = 8$); collagen plus VX-509 50 mg/kg b.i.d. ($n = 8$); collagen plus VX-509 50 mg/kg q.d. ($n = 8$); and collagen plus VX-509 100 mg/kg q.d. ($n = 8$); all treatments were administered for 6 days. An additional group of rats was given collagen plus 10 mg/kg subcutaneous etanercept (provided by Bolder BioPATH), a human tumor necrosis factor-α antagonist, on study days 11 and 14. Caliper measurements of normal (baseline) ankle joints began on day 9 and continued through the last day of study. Differences in mean ankle diameter were tested for significance using Student's t test, with significance set at $P \leq 0.05$. The rats were euthanized on day 7 of arthritis, which was study day 17 or 18 depending on when animals were randomized to groups; paws and knees were harvested to determine paw weight and to conduct a histopathological analysis of inflammation (knee and ankle), pannus formation (ankle), cartilage destruction (knee), and bone resorption (knee and ankle). Scores ranged from 0 (normal) to 5 (severe pathology) and were assigned by a veterinary pathologist. Percent inhibition was calculated using the following formula: [(mean of treatment group) − (mean of control)] ÷ [(mean of collagen + vehicle) − (mean of control)]. Kruskal-Wallis one-way analysis of variance nonparametric tests were used to determine statistical significance among the histopathology groups, with significance set at $P \leq 0.05$.

Pharmacokinetic Analysis. Sampling for pharmacokinetic analysis was done on day 6 of arthritis using six rats per group. Plasma was collected via tail vein from isoflurane-anesthetized rats at 1, 2, 4, 8, and 12 hours postdose. Plasma VX-509 concentrations were determined using a high-performance liquid chromatography (HPLC)–tandem mass spectrometry method. The method is based on 100 μl plasma samples prepared by protein precipitation with addition of 400 μl acetonitrile containing internal standard VRT-125070. Chromatography separation was achieved by reversed-phase HPLC using a 5.0 μm Xterra C18 column (2.1 × 50 mm) and a mobile phase consisting of a mixture of 10 mM ammonium acetate at pH 4.0 in HPLC water and acetonitrile. The lower and upper limits of quantification were 1 and 5000 ng/ml, respectively. A weighting factor of $1/x^2$ was found to suitably describe the relation between analyte concentration and instrument response.

Delayed-Type Hypersensitivity Mouse Model. Male CD-1 mice (Charles River Laboratories) between 6 and 7 weeks old were topically sensitized with either a 5% or 1% (w/v) solution of oxazolone in solvent (1:2 absolute ethanol and acetone) on their shaved abdomens and ears, respectively. Three days after sensitization, mice were challenged with 10 μl 1% oxazolone applied to both sides of the right ear. Solvent alone was applied to both sides of the left ear. For prophylactic dosing, vehicle and VX-509 (10, 25, or 50 mg/kg b.i.d.) or prednisolone (PRED; 5 mg/kg b.i.d., positive control) were administered via oral gavage for 3 days. For therapeutic dosing, doses were initiated 24 hours after oxazolone application. Mice were euthanized 24 hours postchallenge, except for mice in the therapeutic dosing group that were euthanized 48 hours postchallenge. Ear edema was quantified by determining the net increase in weight of the right ear (oxazolone-treated) compared with the left ear (vehicle control), based on 9-mm discs of tissue punched from each of the ears. One-way analysis of variance (ANOVA) with Dunnett's post hoc tests (α set to $P < 0.05$) were used to compare differences between groups.

Results

VX-509 Potently and Selectively Inhibits JAK3 in Biochemical Enzyme Assays. VX-509 inhibited activity of the JAK3 kinase domain potently, with a K_i value of 2.5 ± 0.7 nM (Supplemental Table 3). Of the 79 protein kinases tested, VX-509 also inhibited kinase activity of the other members of the JAK family (JAK1, JAK2, and TYK2) at K_i values of 11, 13, and 11 nM, respectively. The potency of VX-509 against the broad list of counter-screened kinases only produced measurable K_i values for several kinases, all of which had K_i > 1000 nM or > 400-fold selectivity versus JAK3 (Supplemental Tables 3 and 4).

TABLE 3
Percent inhibition, relative to vehicle-treated animals, of ankle diameter, paw weight, and histopathology scores for VX-509 b.i.d. dose experiments

Using ANOVA plus Dunnett's (measures) and Dunn's (scored parameters) post hoc tests. $n = 4$ for naive control group, $n = 5$ for vehicle group, and $n = 8$ for all other treatment groups. Mean baseline values for the collagen + vehicle group are cumulative ankle diameter = 55.9 mm, paw weight = 2.2 g, ankle histopathology score = 10.6, knee histopathology score = 7.7. Control mean baseline values are cumulative ankle diameter = 45.7 mm, paw weight = 1.4 g, ankle histopathology score = 0, knee histopathology score = 0.

Group	Dose	Dosing	Joint Measures, % Inhibition (±S.E.)		Histopathology Score, % Inhibition (±S.E.)	
			Ankle Diameter	Paw Weight	Ankle	Knee
	mg/kg					
Collagen + vehicle	—	b.i.d.	0 (±6.8)	0 (±5)	0 (±12.8)	0 (±18.8)
Collagen + VX-509	10	b.i.d.	55** (±10.3)	65** (±12.8)	59** (±23.4)	81** (±30)
	25	b.i.d.	70** (±5.5)	80** (±8.5)	70** (±12.8)	98** (±6.5)
	50	b.i.d.	76** (±3.4)	93** (±5.5)	81** (±5.3)	100** (±0)
Collagen + etanercept	10	q.4.d.	55** (±9.7)	75** (±9.7)	59** (±18.3)	83** (±28.8)
control	—	—	100**	100**	100**	100**

**$P < 0.01$ compared with CIA rats in the vehicle group.

TABLE 4

Percent inhibition, relative to vehicle-treated animals, of ankle diameter, paw weight, and histopathology scores for VX-509 q.d. dose experiments

Using ANOVA plus Dunnett's (measures) and Kruskal-Wallis ANOVA (scored parameters) post hoc tests. $n = 4$ for control group, $n = 8$ for all treatment groups. Mean baseline values for the collagen + vehicle group are cumulative ankle diameter = 55.9 mm, paw weight = 2.1 g, ankle histopathology score = 11.4, knee histopathology score = 9.3. Control mean baseline values are cumulative ankle diameter = 45.7 mm, paw weight = 1.3 g, ankle histopathology score = 0, knee histopathology score = 0.

Group	Dose	Dosing	Joint Measures, % Inhibition (±S.E.)		Histopathology Score, % Inhibition (±S.E.)	
			Ankle Diameter	Paw Weight	Ankle	Knee
	mg/kg					
Collagen + vehicle	—	q.d.	0 (±7)	0 (±5.5)	0 (±12.5)	0 (±12.9)
Collagen + VX-509	50	q.d.	58** (±7.3)	71** (±9.4)	62** (±16.9)	94** (±3.5)
	100	q.d.	59** (±5.9)	65** (±6)	58** (±7)	100** (±0)
Collagen + etanercept	10	q.4.d.	54** (±7)	70** (±8.2)	61** (±10.1)	84** (±10.9)
Control	—	—	100**	100**	100**	100**

**$P < 0.01$ compared with CIA rats in the vehicle group.

VX-509 Potently Inhibits JAK3 in Cell-Based Assays. JAK3 inhibition by VX-509 was first determined with an IL-2–induced STAT-5 phosphorylation assay in an IL-2–dependent T-cell line (HT-2). The potency of VX-509 for inhibiting JAK3 activity was also assessed in three additional JAK3-dependent assays using primary cells from blood and bone marrow: 1) using an MLR assay, in which splenocytes from two mismatched strains of mice are mixed to trigger T-cell activation; 2) in an IL-2–stimulated blast proliferation assay, in which human peripheral blood mononuclear cells are used to assess inhibition of IL-2–dependent T-cell proliferation; and 3) by quantifying B-cell proliferation in response to CD40L/IL-4.

In the IL-2–stimulated HT-2–phosphorylated STAT-5 fluorescence-activated cell sorting assay, VX-509 had an IC_{50} of 99 ± 40 nM (Table 1). The ability of VX-509 to suppress cytokine-driven immune response was also tested in immune-mediated functional cell assays using both mouse (MLR assay) and human primary cells (T-cell blast proliferation). In the mouse MLR assay, VX-509 potently suppressed T-cell proliferation with a mean IC_{50} of 170 ± 101 nM. In the human T-cell blast proliferation assay, VX-509 also inhibited IL-2–stimulated T-cell proliferation, a measure of JAK3 activity in primary cells (Johnston et al., 1996; Moriggl et al., 1999). The IC_{50} values for VX-509 in this assay were 140 and 400 nM. VX-509 was also assessed for its ability to inhibit B-cell proliferation in response to CD40L and IL-4 (Karras et al., 1997). The IC_{50} of VX-509 for this assay was 50 nM.

VX-509 Demonstrates Limited Inhibition of JAK1/JAK2/TYK2 in Cell-Based Assays. To determine the selectivity of VX-509 for inhibiting different JAK isotypes within cells, cytokine-induced STAT-5 phosphorylation and STAT-2 translocation assays were used. JAK2 inhibition was assessed using a GM-CSF–induced STAT-5 phosphorylation assay in GM-CSF–dependent erythroleukemia (TF-1); and JAK1 and TYK2 inhibition was assessed with an IFN-α–induced STAT-2 translocation assay in HeLa cells. In addition, a human CFU-E assay was performed in the presence of VX-509 to assess its ability to inhibit JAK2-dependent erythrocyte development.

VX-509 was evaluated for potency against JAK1/JAK2/TYK2 in cell-based assays (Table 2). Inhibition of JAK2 by VX-509 was assessed by determining the degree of STAT-5 phosphorylation in the TF-1 human erythroleukemia cell line after stimulation with GM-CSF (Watanabe et al., 1997). The IC_{50} in the TF-1 assay was determined to be 2590 ± 1600 nM (Fig. 2B). Nuclear translocation of STAT-2 in HeLa cells after stimulation with IFN-α was used to measure the effect of VX-509 on the kinase activity of JAK1 and TYK2 (Muller et al., 1993; Darnell et al., 1994). The IC_{50} of VX-509 in the STAT-2 translocation assay was determined to be 11,900 ± 3651 nM. When compared with the IL-2–stimulated γ-chain signaling inhibition in the T-cell line HT-2, VX-509 is ~25-fold less potent in inhibiting JAK2 as determined by the GM-CSF–stimulated TF-1 assay and ~120-fold less potent against JAK1 and TYK2 as measured in the IFN-α–stimulated STAT-2 translocation assay. It is important to note that the specific STATs being measured in these assays were selected because they have been demonstrated to be the predominant and more physiologically relevant STATs used for the specific pathway of interest. For example, using STAT-2 in the IFN-α assay will give more accurate information on the potency than assaying for STAT-3. To extend the evaluation of the JAK isotype selectivity window in more translationally relevant cell-based assays, we measured endpoints in primary cell assays. The mean IC_{50} for VX-509 in the CFU-E assay was 5300–7700 nM, depending on whether 0.3 or 3 U/ml EPO was used in the assay (Table 2). The

TABLE 5

Model independent mean pharmacokinetic parameters for the plasma concentrations obtained on day 6 following oral administration of VX-509 q.d. or b.i.d.; $n = 6$ per dose group

Compound	Regimen	Dose	AUC_{0_12h} (±S.E.)	T_{max} (±S.E.)	C_{max} (±S.E.)	T_{last} (±S.E.)	C_{last} (±S.E.)	$t_{1/2}$ (±S.E.)
		mg/kg	$\mu M \times h$	*h*	μM	*h*	μM	*h*
VX-509	b.i.d.	10	10.8 (±3.6)	1 (±0.33)	3.4 (±1,3)	12 (±0)	0.2 (±0.05)	3.12 (±1.6)
VX-509	b.i.d.	25	21.4 (±4.5)	1 (±0)	7.2 (±1.8)	12 (±0)	0.2 (±0.07)	2.2 (±0.1)
VX-509	b.i.d.	50	71.1 (±7.8)	1 (±0.3)	12.1 (±1.1)	12 (±0)	0.6 (±0.2)	2.4 (±0.4)
VX-509	q.d.	50	102.5 (±0.6)	1 (±0.3)	19.3 (±1.2)	12 (±0)	0.5 (±0.2)	1.94 (±0.2)
VX-509	q.d.	100	170.5 (±7.4)	1 (±0)	33.6 (±5)	12 (±0)	2.7 (±0.9)	3.15 (±0.8)

AUC, area under the curve; C_{last}, concentration at last measurement; T_{last}, time at last measurement.

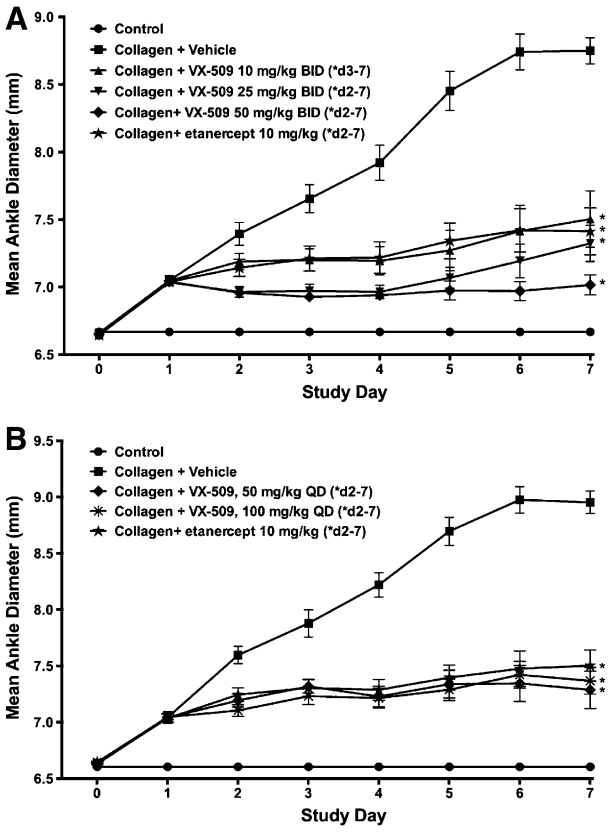

Fig. 2. Effect of VX-509 on progression of established disease in rat CIA model. At onset of paw swelling (established disease), the rats were randomized into the various study groups. Dosing was initiated on first day of established disease and continued for 6 days. Ankle diameter was measured over a 7-day study period in the CIA model. Graphs depict group mean ankle diameter during the study. Groups were given vehicle, VX-509, or etanercept (10 mg/kg). Error bars are ± S.E.M. $n = 4$ rats in each of the control groups; $n = 8$ rats per treatment group. *$P < 0.05$ based on Student's t tests. (A) Rats were administered VX-509 in a b.i.d. dosing regimen at 10, 25, or 50 mg/kg. All treatment groups were significantly lower than the vehicle-treated group. (B) Rats were administered VX-509 in a q.d. dosing regimen at 50 or 10 mg/kg. All treatment groups were significantly lower than the vehicle-treated group.

MLR/CFU-E IC_{50} ratio for VX-509 was determined to be ~30- to 45-fold.

VX-509 Suppresses Joint Inflammation in a Rat Model of Collagen-Induced Arthritis. The CIA model shares a number of pathologic, genetic, and immunologic features with RA. Type II collagen (CII) is a major component of articular cartilage, and several studies have demonstrated that the presence of T-cell and B-cell infiltrates underlies immune reactions to CII in patients with RA. In rodents, injection with CII also induces inflammation in the joints and leads to cartilage destruction and bone resorption. VX-509 showed statistically significant, dose-dependent inhibition of the increases in ankle diameter and paw weight that occur in response to collagen injections in rats treated with VX-509 b.i.d. at doses of 10, 25, or 50 mg/kg or etanercept at 10 mg/kg (Table 3). A significant decrease, according to Student's t test, in ankle diameter was seen in rats treated orally with VX-509 10 mg/kg b.i.d. (days 3–7), 25 mg/kg b.i.d. (days 2–7), 50 mg/kg b.i.d. (days 2–7), or 10 mg/kg etanercept (days 2-7) as compared with collagen plus vehicle controls ($P \leq 0.05$) (Fig. 2A). Inhibition of ankle diameter increase was significant (ANOVA with Dunnett's post hoc tests) for rats treated with VX-509 at 10 mg/kg b.i.d. (55% inhibition), 25 mg/kg b.i.d. (70% inhibition), 50 mg/kg b.i.d. (76% inhibition), or 10 mg/kg etancercept (55% inhibition) relative to collagen plus vehicle-treated rats ($P < 0.01$) (Table 3). Final paw weight increases were significantly (ANOVA, $P \leq 0.05$) lower in rats treated with VX-509 at 10 mg/kg b.i.d. (65% inhibition), 25 mg/kg b.i.d. (80% inhibition), 50 mg/kg b.i.d. (93%), or 10 mg/kg etancercept (75%) relative to collagen plus vehicle-treated rats ($P < 0.01$) (Table 3).

VX-509 was also evaluated with once daily dosing (q.d.) and showed a statistically significant, dose-dependent decrease in ankle diameter and paw weight. Significant inhibition of ankle diameter increase was seen in rats treated with VX-509 at 50 mg/kg q.d. (days 2–7), 100 mg/kg q.d. (days 2–7), or 10 mg/kg etanercept (days 2–7) compared with rats in the collagen plus vehicle-treated group (Student's t test, $P < 0.05$) (Fig. 2B). Inhibition of increases in ankle diameter was significant for rats administered VX-509

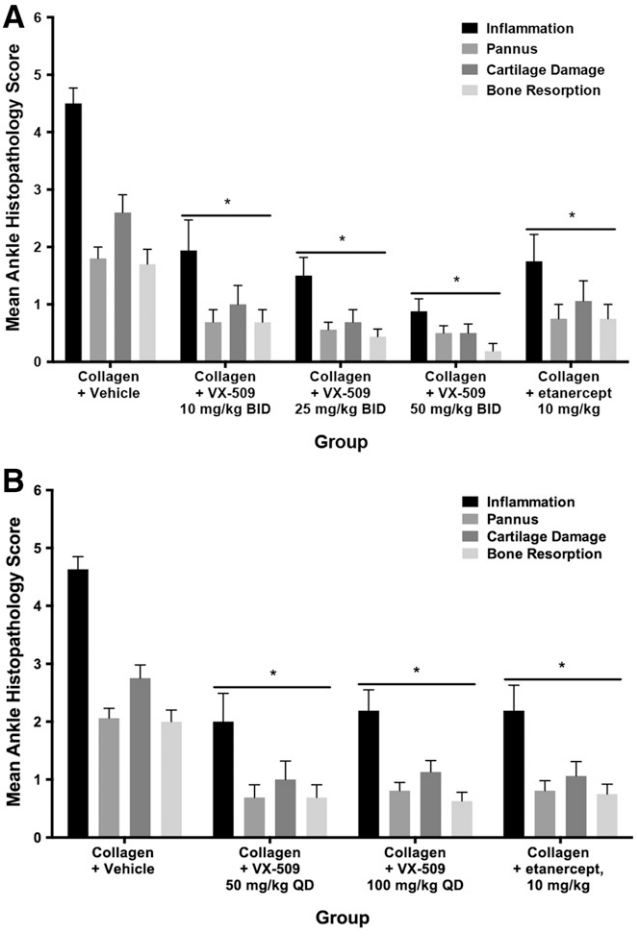

Fig. 3. Joints were evaluated by histopathology stained with H&E. Sections were scored for inflammation, pannus formation, cartilage damage, and bone resorption. Graphs depict the group mean histopathology scores in the various categories. $n = 8$ rats/treatment group; $n = 5$ rats in control group. (A) b.i.d. dosing of VX-509 at 10, 25, or 50 mg/kg effectively protects ankles from inflammation, pannus formation, and cartilage and bone damage in the rat CIA model. *$P \leq 0.05$ relative to vehicle control, using Dunnett's post hoc tests. (B) q.d. dosing of VX-509 at 50 or 100 mg/kg effectively protects ankles from inflammation, pannus formation, and cartilage and bone damage in the rat CIA model. *$P \leq 0.05$ relative to vehicle control, using Kruskal-Wallis one-way analysis of variance.

at 50 mg/kg q.d. (58% inhibition), 100 mg/kg q.d. (59% inhibition), or 10 mg/kg etancercept (54% inhibition) (Table 4) (ANOVA, $P \leq 0.01$). The inhibition of paw weight increases was significant for rats treated with VX-509 at 50 mg/kg q.d. (71% inhibition), 100 mg/kg q.d. (65% inhibition), and etanercept at 10 mg/kg (70% inhibition) (ANOVA, $P \leq 0.05$) relative to rats from the collagen plus vehicle group (Table 4).

Additionally, mean ankle histopathology scores (including inflammation, pannus, cartilage damage, and bone resorption) were significantly reduced in rats treated with VX-509 either b.i.d. or q.d. compared with animals in the vehicle

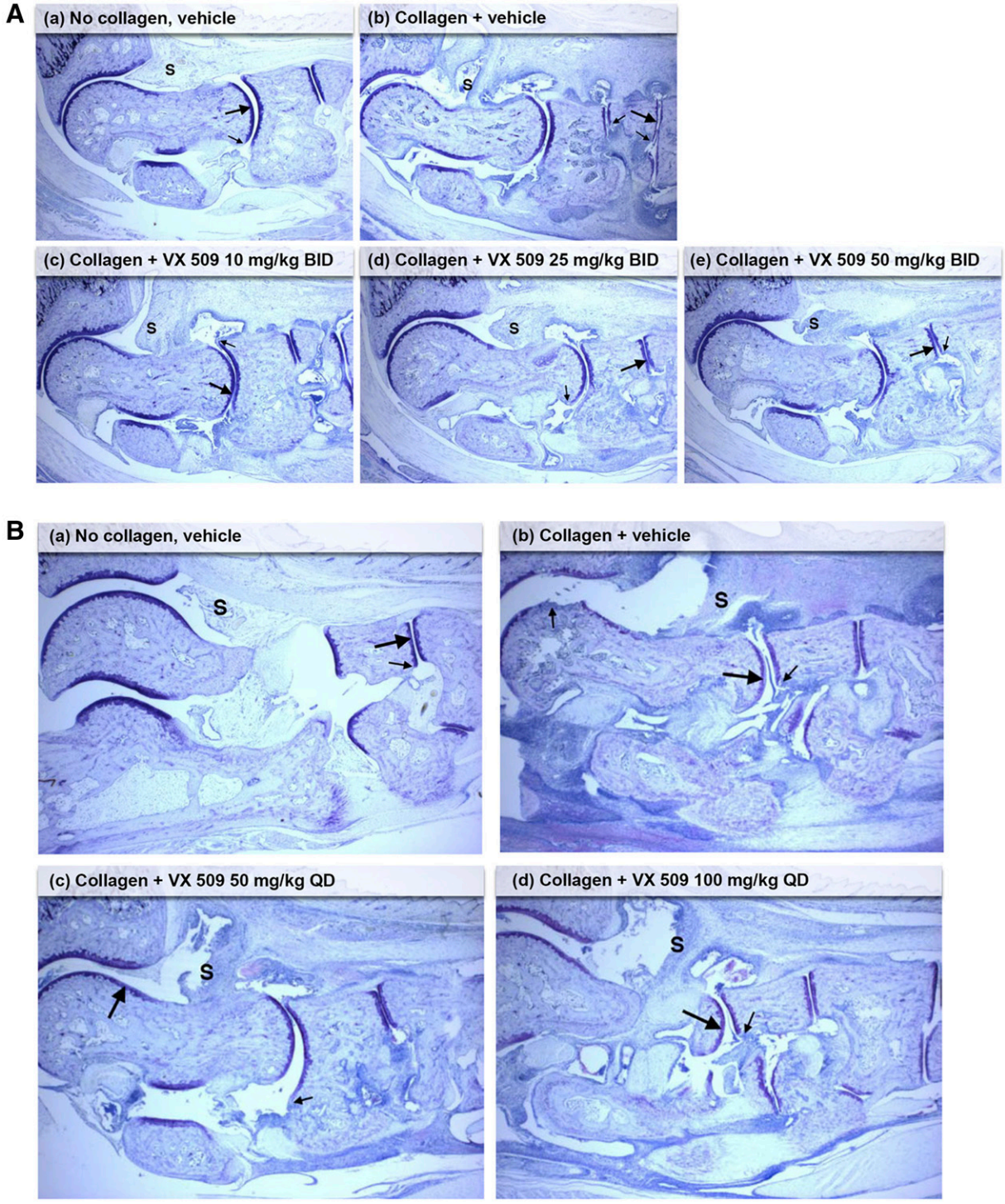

Fig. 4. (A) Representative histopathology photomicrographs of a control (collagen + vehicle) rat ankle and VX-509 b.i.d. treatment groups, with approximate mean score for group showing synovium (S), cartilage (large arrow), and bone (small arrow). Group size for histology analysis are $n = 8$ rats/treatment group, 5 rats in control group. (B) Representative histopathology photomicrographs of a control (collagen + vehicle) rat ankle and VX-509 q.d. treatment groups, with approximate mean score for group showing synovium (S), cartilage (large arrow), and bone (small arrow). Group size for histology analysis are $n = 8$ rats/treatment group, 5 rats in control group.

group (Fig. 3). Rats administered vehicle alone showed marked synovitis and periarticular inflammation in ankles, with mild infiltration of pannus, bone resorption, and cartilage damage. Rats in the VX-509 groups had significantly less ($P \leq 0.01$) cartilage damage and bone resorption at all doses of VX-509 tested (Figs. 3 and 4, A and B).

In both studies, VX-509 showed a dose-dependent increase in exposure. The exposure achieved with b.i.d. dosing and q.d. dosing is shown in Fig. 5 and summarized in Table 5. The maximum measured levels of VX-509 at 10, 25, and 50 mg/kg b.i.d. doses were 1.3, 2.8, and 4.7 μg/ml, respectively. Similarly, the maximal drug concentrations at 50 and 100 mg/kg q.d. were 7.6 and 13.2 μg/ml, respectively. Drug exposure levels were above the cellular IC_{50} in the JAK3-dependent cell assays for all doses throughout the duration of the dose interval while below or near the IC_{50} of JAK1/2/TYK2-dependent cell assays. This suggests inhibition of JAK3 primarily accounts for the physiologic effects of VX-509 in the CIA model. Additionally, this exposure/selectivity analysis was confirmed and extended with the JAK3 versus JAK1/2-dependent biomarker assays from phase I studies conducted with VX-509 in healthy human volunteers (Catlett et al., 2012). Based on these studies, the EC_{50} for JAK3-induced pSTAT5 inhibition was seen at 0.55 μg/ml. This concentration produced no significant effect in the JAK1/2-induced pSTAT3 phase 1 biomarker assay. Furthermore, only partial inhibition (~50%) was observed in this assay at the highest dose levels tested in these studies.

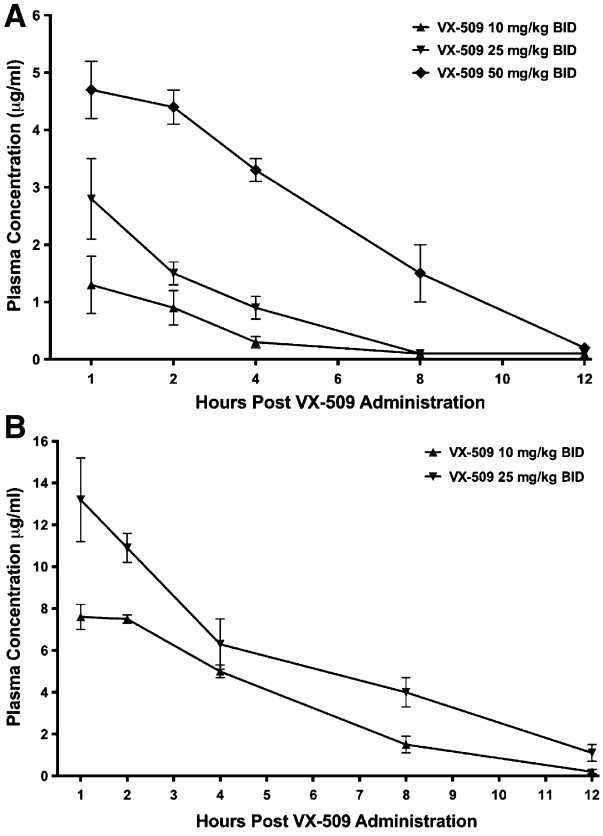

Fig. 5. Plasma VX-509 concentrations in the CIA study. (A) Day 6 plasma levels (micrograms per milliliter) after b.i.d. VX-509 administration in CIA rats (n = 3 at each time point). (B) Day 6 plasma levels (micrograms per milliliter) after q.d. VX-509 administration in CIA rats (n = 3 at each time point).

VX-509 Suppresses Ear Edema in a Mouse Model of Delayed-Type Hypersensitivity. The mouse oxazolone-induced delayed-type hypersensitivity (DTH) model produces epidermal hyperplasia and reactive T-cell infiltration leading to pathologic events that are believed to be important in the etiology of psoriasis and allergic contact dermatitis. The DTH model has been useful for evaluating the effects of test compounds on skin inflammation, reflecting cell-mediated immunity. In the DTH model, VX-509 at doses of 10, 25, or 50 mg/kg b.i.d. significantly inhibited T cell–mediated ear edema when administered either prophylactically (Fig. 6A) or therapeutically (Fig. 6B). Figure 6A (prophylactic dosing) shows that VX-509 significantly suppressed ear edema by 28.8% in the VX-509 25 mg/kg b.i.d. group ($P < 0.01$) and by 43.5% in the VX-509 50 mg/kg b.i.d. group ($P < 0.01$) compared with ears in vehicle-treated animals. The mean increase in ear weight was not significantly different among mice treated with VX-509 25 mg/kg b.i.d., 50 mg/kg b.i.d., or PRED 5 mg/kg q.d.

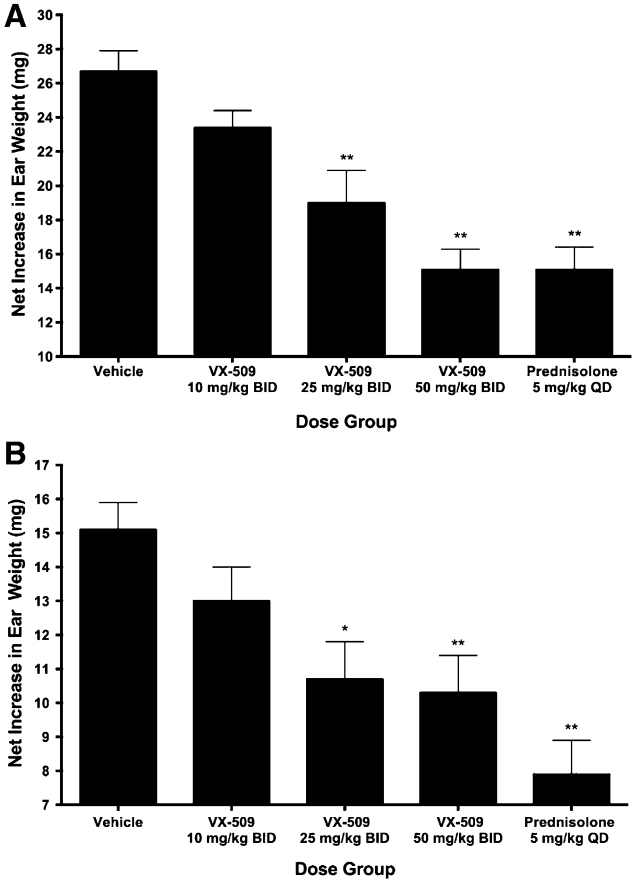

Fig. 6. Effect of VX-509 on the oxazolone-induced mouse DTH model. Mice were sensitized with 5% oxazolone solution applied to shaved abdomen. Mice were challenged on day 3 with 1% oxazolone solution on right ear; solvent alone was applied to left ear as control. For prophylactic dosing, vehicle or compounds were administered on day 3 prior to oxazolone challenge; for therapeutic dosing, vehicle or compounds were administered 24 hours after oxazolone challenge. n = 7 for all vehicle and treatment groups. (A) When dosed prophylactically, VX-509 significantly suppresses ear edema. ANOVA followed by Dunnett's post hoc tests for comparisons with vehicle control. $^*P \leq 0.05$, $^{**}P \leq 0.01$. (B) When using a therapeutic dosing regimen, VX-509 significantly suppresses ear edema. ANOVA followed by Dunnett's post hoc tests for comparisons with vehicle control: $^*P \leq 0.05$, $^{**}P \leq 0.01$.

When the DTH model was evaluated using a therapeutic dosing regimen (dosed 24 hours postchallenge), there was a 13.9% inhibition in ear edema in the VX-509 10 mg/kg b.i.d. group (N.S.), a 29.1% inhibition in the VX-509 25 mg/kg b.i.d. group ($P < 0.05$), and a 31.8% inhibition in the VX-509 50 mg/kg b.i.d. group ($P < 0.01$). Ear edema was decreased by 47.7% ($P < 0.01$) in mice treated with PRED at 5 mg/kg q.d. ($P \leq 0.001$), which was not significantly different from the reduction in edema in the VX-509 50 mg/kg b.i.d. group.

Discussion

JAK3 is a key enzyme in the immune-signaling cascade that underlies both host defense and the pathophysiology of a variety of autoimmune diseases (Ghoreschi et al., 2009; O'Shea and Plenge, 2012). Because JAK3 expression is largely restricted to lymphocytes (O'Shea and Plenge, 2012), a selective JAK3 inhibitor may have promise for reducing immune-mediated inflammation in vivo. In this study, in vitro assays confirmed that VX-509 is a potent and selective inhibitor of JAK3 and that it effectively reduces the development of immune-mediated pathologies in two animal models of autoimmune disease.

The data from these studies show that VX-509 is a potent inhibitor of JAK3-associated events in cells and that it is selective over other JAK isotypes. Importantly, selectivity was shown against JAK2, the most closely related JAK family member to JAK3 (Menet et al., 2013). Compared with the T-cell proliferation response in primary human and mouse cells, we observed a 45-fold reduction in potency when compared with CFU-E assays using human bone marrow stimulated with EPO. Additionally, VX-509 is a potent suppressor of B-cell activation as measured by CD40/IL-4 stimulation of primary human B cells, which is important given that B cells are the source of autoantibodies such as rheumatoid factor that lead to immune complex formation and complement activation in RA (McInnes and Schett, 2011).

Animal pharmacology studies shown in this work demonstrate that VX-509 effectively reduced inflammation and its associated pathologies in the rat CIA model. VX-509 also demonstrated inhibition of physiologic processes that have been shown to underlie RA disease progression in humans, including cartilage damage and bone resorption (McInnes and Schett, 2011). The findings from the DTH model, which is used to model the effects of compounds prior to clinical studies (Stevenson et al., 2006), indicate that VX-509 quickly and dose-dependently inhibits a T cell–mediated inflammatory process. Interestingly, with only a single day of VX-509 administration, after the swelling of ear tissue had already occurred, significant reduction of immune cell infiltration and edema was observed. Although speculative, the rapidity of therapeutic response in this model indicates the possibility that therapeutic effect by VX-509 could be rapid in humans as well.

Stable full-length JAK proteins are extraordinarily difficult to produce and use in enzyme-based assays. To facilitate medicinal chemistry strategy and to ultimately characterize VX-509, we instead used the isolated activated kinase domain as a substitute for the full-length protein. These enzyme assays did allow for rapid and approximate measures of potency for the four JAK isotypes. Additional kinase selectivity shows that against a broad panel of non-JAK kinases, VX-509 is selective. For a more biologically informative measure of the JAK isotype potency and selectivity of VX-509, we used a series of cell-based assays that measured either the direct substrate (e.g., phosphorylation of STAT proteins) or more physiologically important endpoints measured in primary human and mouse cells (e.g., T-cell proliferation response). The homology of the ATP-binding pocket for the JAK isotypes is nearly identical between humans and mice, making data from both cell sources informative. Ultimately, we relied on the primary cell-based assays, given their increased biologic relevance when compared with isolated proteins in vitro, to determine the JAK isotype selectivity window for VX-509. These data suggest that we will be able to interrogate JAK3 inhibition in the context of a clinical study with confidence that we are not inhibiting the other JAK isotypes to a significant degree.

A key advantage of selectively targeting JAK3 as a therapy for a variety of autoimmune diseases is that its expression is largely restricted to lymphocytes and its physiologic effects are limited to signals from the common γ-chain family of cytokine receptors (Johnston et al., 1996). Other members of the JAK family have a much broader tissue expression pattern and are involved in a wider array of physiologies. For example, in addition to hematopoietic and growth factor signaling, JAK2 also plays an essential role in the gp130 class and the IFN-γ receptor signaling pathways (Kiu and Nicholson, 2012). JAK1 is also broadly used, not only by the common γ-chain receptors along with JAK3, but also by gp130 receptors, where it pairs with JAK2, and also in both type I, II, and III IFN signaling (Kiu and Nicholson, 2012). Thus, inhibition of JAK1 will have the same impact on the γ-chain cytokines as inhibitors of JAK3, but will also include consequence of the inhibition of the gp130 and IFN signaling responses. At the 10 mg/kg dose level in the CIA model, VX-509 produced significant inhibition of the immune-mediated pathology with exposure levels above the IC_{50} point for JAK3 while below the IC_{50} points for the JAK2/JAK1/TYK2 assays. Results from these preclinical studies demonstrate that VX-509 is a selective JAK3 inhibitor, and selective JAK3 inhibition is sufficient for reducing pathology in animal models of autoimmune disease. Finally, given the selectivity profile of VX-509, avoiding chronic and systemic suppression of the other JAK isotypes may lead to meaningful clinical differences in safety and tolerability (e.g., anemia), making VX-509 an attractive candidate for evaluation in clinical studies of autoimmune diseases such as RA.

Acknowledgments

The authors thank the VX-509 project team for helping to advance this compound into clinical development.

Authorship Contributions

Participated in research design: Mahajan, Hogan, Shlyakhter, Oh, Salituro, Farmer, Hoock.

Conducted experiments: Mahajan, Hogan, Shlyakhter, Oh.

Contributed new reagents or analytic tools: Farmer.

Performed data analysis: Mahajan, Hogan, Shlyakhter, Oh, Hoock.

Wrote or contributed to the writing of the manuscript: Mahajan, Hogan, Shlyakhter, Oh, Salituro, Farmer, Hoock.

References

Cacalano NA, Migone TS, Bazan F, Hanson EP, Chen M, Candotti F, O'Shea JJ, and Johnston JA (1999) Autosomal SCID caused by a point mutation in the N-terminus of Jak3: mapping of the Jak3-receptor interaction domain. *EMBO J* **18**: 1549–1558.

Carmona L, Cross M, Williams B, Lassere M, and March L (2010) Rheumatoid arthritis. *Best Pract Res Clin Rheumatol* **24**:733–745.

Catlett, IM, Luo X, Penney MS, Pray ME, Spencer-Green G, Botfield M, and Hoock T (2012) Biomarker Assessment of VX-509, an Investigational Selective Inhibitor, in

Healthy Volunteers. *European League Against Rheumatism (EULAR) Congress*; 2012 Jun 6–9; Berlin, Germany. EULAR Poster 2012 (THU0141).
Chen G, Porter MD, Bristol JR, Fitzgibbon MJ, and Pazhanisamy S (2000) Kinetic mechanism of the p38-alpha MAP kinase: phosphoryl transfer to synthetic peptides. *Biochemistry* **39**:2079–2087.
Darnell JE, Jr (1997) STATs and gene regulation. *Science* **277**:1630–1635.
Darnell JE, Jr, Kerr IM, and Stark GR (1994) Jak-STAT pathways and transcriptional activation in response to IFNs and other extracellular signaling proteins. *Science* **264**:1415–1421.
Davies SP, Reddy H, Caivano M, and Cohen P (2000) Specificity and mechanism of action of some commonly used protein kinase inhibitors. *Biochem J* **351**:95–105.
Ghoreschi K, Laurence A, and O'Shea JJ (2009) Janus kinases in immune cell signaling. *Immunol Rev* **228**:273–287.
Grossman WJ, Verbsky JW, Yang L, Berg LJ, Fields LE, Chaplin DD, and Ratner L (1999) Dysregulated myelopoiesis in mice lacking Jak3. *Blood* **94**:932–939.
Ihle JN and Kerr IM (1995) Jaks and Stats in signaling by the cytokine receptor superfamily. *Trends Genet* **11**:69–74.
Johnston JA, Bacon CM, Riedy MC, and O'Shea JJ (1996) Signaling by IL-2 and related cytokines: JAKs, STATs, and relationship to immunodeficiency. *J Leukoc Biol* **60**:441–452.
Karras JG, Wang Z, Huo L, Frank DA, and Rothstein TL (1997) Induction of STAT protein signaling through the CD40 receptor in B lymphocytes: distinct STAT activation following surface Ig and CD40 receptor engagement. *J Immunol* **159**:4350–4355.
Kiu H and Nicholson SE (2012) Biology and significance of the JAK/STAT signalling pathways. *Growth Factors* **30**:88–106.
Macchi P, Villa A, Giliani S, Sacco MG, Frattini A, Porta F, Ugazio AG, Johnston JA, Candotti F, O'Shea JJ, et al. (1995) Mutations of Jak-3 gene in patients with autosomal severe combined immune deficiency (SCID). *Nature* **377**:65–68.
McInnes IB and Schett G (2011) The pathogenesis of rheumatoid arthritis. *N Engl J Med* **365**:2205–2219.
Menet CJ, Rompaey LV, and Geney R (2013) Advances in the discovery of selective JAK inhibitors. *Prog Med Chem* **52**:153–223.
Moriggl R, Topham DJ, Teglund S, Sexl V, McKay C, Wang D, Hoffmeyer A, van Deursen J, Sangster MY, Bunting KD, et al. (1999) Stat5 is required for IL-2-induced cell cycle progression of peripheral T cells. *Immunity* **10**:249–259.
Müller M, Briscoe J, Laxton C, Guschin D, Ziemiecki A, Silvennoinen O, Harpur AG, Barbieri G, Witthuhn BA, Schindler C, et al. (1993) The protein tyrosine kinase JAK1 complements defects in interferon-alpha/beta and -gamma signal transduction. *Nature* **366**:129–135.
Neubauer H, Cumano A, Müller M, Wu H, Huffstadt U, and Pfeffer K (1998) Jak2 deficiency defines an essential developmental checkpoint in definitive hematopoiesis. *Cell* **93**:397–409.
Nosaka T, van Deursen JM, Tripp RA, Thierfelder WE, Witthuhn BA, McMickle AP, Doherty PC, Grosveld GC, and Ihle JN (1995) Defective lymphoid development in mice lacking Jak3. *Science* **270**:800–802.
O'Shea JJ and Plenge R (2012) JAK and STAT signaling molecules in immunoregulation and immune-mediated disease. *Immunity* **36**:542–550.
Parganas E, Wang D, Stravopodis D, Topham DJ, Marine JC, Teglund S, Vanin EF, Bodner S, Colamonici OR, van Deursen JM, et al. (1998) Jak2 is essential for signaling through a variety of cytokine receptors. *Cell* **93**:385–395.
Park SY, Saijo K, Takahashi T, Osawa M, Arase H, Hirayama N, Miyake K, Nakauchi H, Shirasawa T, and Saito T (1995) Developmental defects of lymphoid cells in Jak3 kinase-deficient mice. *Immunity* **3**:771–782.
Rodig SJ, Meraz MA, White JM, Lampe PA, Riley JK, Arthur CD, King KL, Sheehan KC, Yin L, Pennica D, et al. (1998) Disruption of the Jak1 gene demonstrates obligatory and nonredundant roles of the Jaks in cytokine-induced biologic responses. *Cell* **93**:373–383.
Russell SM, Tayebi N, Nakajima H, Riedy MC, Roberts JL, Aman MJ, Migone TS, Noguchi M, Markert ML, Buckley RH, et al. (1995) Mutation of Jak3 in a patient with SCID: essential role of Jak3 in lymphoid development. *Science* **270**:797–800.
Stark GR and Darnell JE, Jr (2012) The JAK-STAT pathway at twenty. *Immunity* **36**:503–514.
Stevenson CS, Marshall LA, and Morgan DW, editors (2006) *In Vivo Models of Inflammation: Progress in Inflammation Research*, Birkhäuser, Basel.
Taylor N, Uribe L, Smith S, Jahn T, Kohn DB, and Weinberg K (1996) Correction of interleukin-2 receptor function in X-SCID lymphoblastoid cells by retrovirally mediated transfer of the gamma-c gene. *Blood* **87**:3103–3107.
Watanabe S, Itoh T, and Arai K (1997) Roles of JAK kinase in human GM-CSF receptor signals. *Leukemia* **11** (Suppl 3):76–78.

Address correspondence to: Dr. Thomas C. Hoock, Vertex Pharmaceuticals, 50 Northern Avenue, Boston, MA 02210. E-mail: Thomas_hoock@vrtx.com